HIGH-SPEED ELECTROSTATIC MICRO-HYDRAULICS FOR SENSING AND ACTUATION

Mahdi M. Sadeghi, Rebecca L. Peterson, and Khalil Najafi
Center for Wireless Integrated Micro Sensing and Systems (WIMS²)
University of Michigan, Ann Arbor, MI, USA

ABSTRACT

In this paper, we report a novel architecture for significant performance enhancement of previously introduced electrostatic micro-hydraulic structures. We develop a 2-D multi-physics model for analysis of our first generation electrostatic micro-hydraulic system (*straight-wall* architecture) used for sensing and actuation. Using this model, we design and fabricate a new *sloped-wall* device with a time constant 400× less than that of earlier designs, while maintaining other specification. The optimized electrostatic micro-hydraulic systems are successfully fabricated and tested. Micro-hydraulic structures of various geometries exhibit a measured bandwidth of 50 to 70 Hz, which corresponds to a sensor response time of about 18 ms.

INTRODUCTION

Actuators that can provide high-force or large-deflection are critical for devices such as valves and pumps used in microfluidic systems, for surface bump manipulation in tactile displays, and for micro-airfoil control. However direct electrostatic actuation cannot provide the high force (~10-100 mN) and high deflection (tens of µm) required for many applications. Other conventional high force mechanisms suffer from high power (e.g. electromagnetic) or process integration issues (e.g. piezoelectric). Hydraulic, (i.e. fluidic or pneumatic) methods are widely used on the macro scale to amplify force or deflection. However most micro-hydraulic systems depend on an external source of actuation, suffer from challenging liquid encapsulation techniques, are not suitable for parallel micro-fabrication processes or exhibit poor performance such as cross talk between adjacent cells in an array [1]. We have previously shown that we can address these challenges by combining electrostatic actuation with hydraulic amplification to achieve either large deflection or high force [2]. The devices are realized using a wafer-level liquid encapsulation technology [3]. Electrostatic sensing using a micro-hydraulic structure is also beneficial because it decouples dynamic range from sensitivity. Additionally, the sensor base capacitance increases due to the larger liquid relative dielectric constant within the electrostatic gap. The enclosed capacitive gap is also more robust due to reduced environmental exposure. These features enable a new class of sensors with large dynamic range and high sensitivity. A variety of sensors can be realized by integration of an appendage that specifically functionalizes the micro-hydraulic chip, such as micro-hydraulic hair air flow sensors [4], or tactile sensors [5].

Consequently, micro-hydraulics combined with electrostatic sensing or actuation offers a new route to high-performance MEMS. However, our and other groups' previously reported micro-hydraulic devices have relatively slow response times on the order of a few seconds, and thus cannot provide the moderate bandwidths (~10s Hz) needed for some MEMS applications [1, 4-7]. Here we use simulations and models to understand the bottlenecks that limit system speed. We use the models to design a new high-speed electrostatic micro-hydraulic architecture for sensors and actuators. The models and analytical techniques can be applied to other systems to improve their performance.

MODELING, SIMULATION AND DESIGN

Straight-wall vs. Sloped-wall

Figure 1 (top) shows a cross-sectional diagram of the *straight-wall* electrostatic micro-hydraulic device, which has been described elsewhere in detail [2, 4, 7]. It consists of top and bottom hydraulic chambers (made by Si recess) connected by a straight-wall channel, all filled with incompressible fluid (here, silicone oil) and encapsulated by flexible top/bottom parylene membranes. In order to determine the dominant contribution to device delay, we developed a 2-D multi-physics model in COMSOL. The model uses three linked modules: structural mechanics (*Plain Strain*), *Moving Mesh* and fluidics (*Incompressible Navier-Stokes*). *Moving mesh* is used since we have observed large deflection of the top membrane [3]. In order to simulate the response time, a step pressure is applied on the backside membrane and the deflection in the center of the front side membrane is monitored. The geometry and physical properties used in the analysis of the *straight-wall* architecture are listed in Table 1.

The rise time of front-side membrane deflection is simulated in response to a step change in backside pressure, for various fluids (Figure 2). Air is assumed to be incompressible. The response time scales with fluid viscosity, ranging from 20s for silicone oil to 4 ms for air, showing that Poiseuille flow [8] in the channel connecting the chambers is the dominant component governing fluid dynamics.

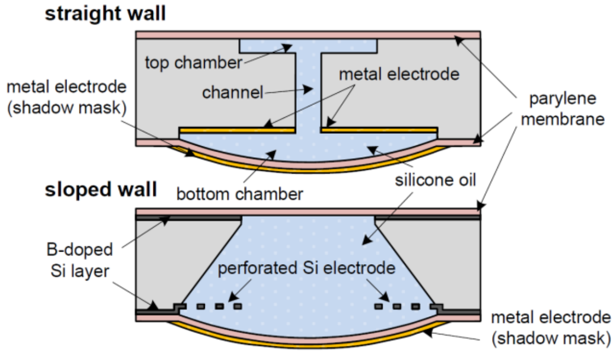

Figure 1: Schematic cross section view of straight- and sloped-wall micro-hydraulic structures.

Table 1: Parameters used for simulation of straight-wall micro-hydraulic device.

Fluid Viscosity at 25˚C	Silicone oil	175 cSt
	Water	1 cSt
	Air	0.0178 cSt
Device Geometry	Front side chamber depth	10 µm
	Back side chamber depth	5 µm
	Parylene membrane thickness	1 µm
	Channel width	200 µm
	Front side membrane width	1 mm
	Back side membrane width	2 mm

The fluidic resistance, R_f, is given by $R_f = (128/\pi)\cdot\mu L D^{-4}$, where μ is the dynamic viscosity of the fluid, and L and D are the length and hydraulic diameter of the channel, respectively [8]. As expected, fluidic resistance is highly dependent on the channel diameter. In order to remove any additional resistance caused by the narrow gap between the front side membrane and the front side recess, we eliminate the recess and silicon underneath and introduce a new design geometry, which we refer to as *sloped-wall* channel (Figure 1, bottom). In going from the *straight-wall* to the ideal *sloped-wall* geometry, the larger effective channel diameter causes a > 6,000× reduction in the response time of the micro-hydraulic device with silicone oil, from 20 s to 3 ms (Figure 2).

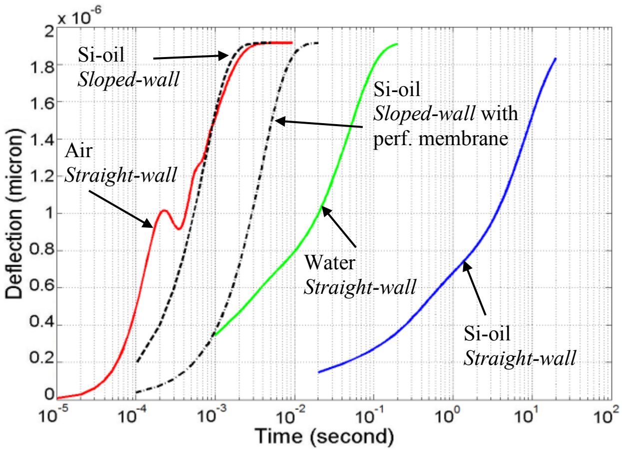

Figure 2: Simulation results comparing step response of fluids with various viscosities using straight-wall geometry, and comparing silicone oil response for three architectures: straight-wall, sloped-wall, and sloped-wall with perforated membrane.

In the straight-wall architecture, electrostatic sense/actuation of the backside membrane was achieved using a metal electrode on the Si recess (Figure 1, top) and the second metal film on the flexible parylene membrane. However, the *sloped-wall* design does not provide a location for this electrode as the silicon bulk is removed to improve the speed of the device. Therefore we add a suspended perforated electrode as shown in Figure 1. The perforated electrode slightly increases the predicted response time from 3ms (with no membrane) to 20ms, as shown in Figure 2. Nonetheless, the overall improvement in transient behavior with the re-designed architecture is 1000× better. The perforated membrane has a large center hole with a diameter the same as the channel width in the straight wall architecture. For the simulations in Figure 2, the perforated section of this membrane consists of 20 µm wide, 10 µm thick silicon blocks with spacing of 20 µm.

Optimization of the Perforated Membrane

The perforation size and pattern must be chosen to co-optimize rise-time (which favors no membrane) and capacitance (which favors a solid membrane). We have modeled this using COMSOL. Figure 3 (top) shows simulated change in capacitance vs. perforation ratio in the perforated electrode. To model this, the bottom electrode is divided into 50 pieces (the bottom electrode diameter is 4 mm in this simulation, so each block has a width of 80 µm) and perforation ratio – defined as the ratio of the perforation opening to the pitch size - is changed. Due to large fringing fields, the perforation ratio can be high (94%) without incurring significant (> 20%) reduction in base capacitance.

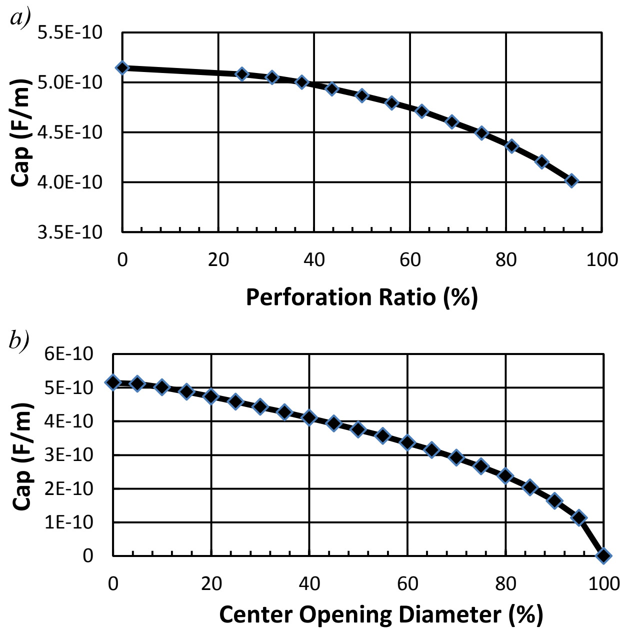

Figure 3: a) Total capacitance vs. perforation ratio. Perforation ratio is the perforation opening size divided by the perforation pitch, here 80µm. b) Capacitance change versus center opening diameter, given as a percentage of the membrane diameter, here 4mm.

Figure 3b shows simulated capacitance vs. center opening size, stated as a fraction of the membrane diameter. A capacitance change of ~ 100 pF occurs when the opening widens from 0 to 40%, and when the opening changes from 95% to 100% of the diameter. This illustrates that, due to the curvature of the electrode on the parylene membrane, the perimeter of the capacitor disproportionately contributes to total capacitance. Therefore, a large center hole can be added to aid fluid flow. Based on these analyses, we choose opening diameter and perforation opening ratio of 55-65% and 90%, respectively.

Time Response Symmetry vs. Parylene Thickness

Simulations also show that the system parameters that affect rise time and fall time are different: rise time is set by fluid viscosity while fall time is determined by membrane elasticity. To model the use of micro-hydraulic in the sensing mode, we simulate the deflection of the front-side membrane with a step pressure and monitor the resulting deflection of the backside membrane. Simulation results show that the dominant rise-time component is hydraulic delay, while parylene membrane elasticity dominates the fall-time. As shown in Figure 4, a change in the membrane thickness increases its moment of inertia, which reduces the fall time and maximum deflection. For the device geometry modeled here, a 2 µm thick parylene film results in a symmetric time response.

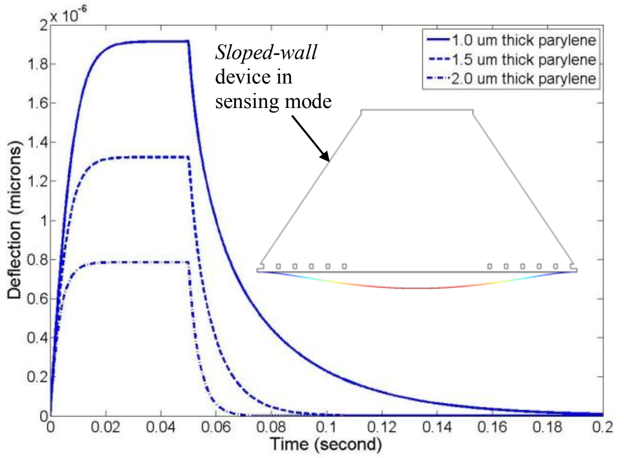

Figure 4: Simulated rise and fall of the backside membrane in response to pulsed pressure on the front side, i.e. simulated sensor operation. The inset shows a snapshot of the COMSOL model with sloped-wall and perforated membrane.

FABRICATION

Figure 5 schematically shows the fabrication process. It starts with the definition of a backside recess by DRIE, followed by deep boron diffusion. This recess determines the capacitance gap. The deep boron diffused layer has a thickness of about 13 µm. The perforation pattern and front side chamber's opening are DRIE etched 20 µm deep through this layer on the front and back sides, followed by EDP to etch the channel and release the electrode while other features on the front side are protected with a blanket oxide layer. Perforated patterns are designed in a way that the anisotropically-etched pyramid under each opening overlaps with adjacent ones to fully release the electrode and form sloped wall channels. After EDP etching step, the protective oxide layer is stripped in HF. Hydrophobic Cytop^{TM} layer is then formed and patterned on both sides [2]. This layer repels the silicone fluid so that the oil will be contained in Cytop^{TM} free areas. The silicone oil (1,3,5-trimethyl-1,1,3,5,5-pentaphenyltrisiloxane) is dispensed and kept in place due to surface tension and hydrophobic Cytop^{TM} layer. This particular silicone oil has a very low vapor pressure, so it does not evaporate inside the parylene deposition vacuum chamber. Once the oil is dispensed on the wafer, in a single deposition run, a 2µm parylene layer encapsulates the silicone liquid.

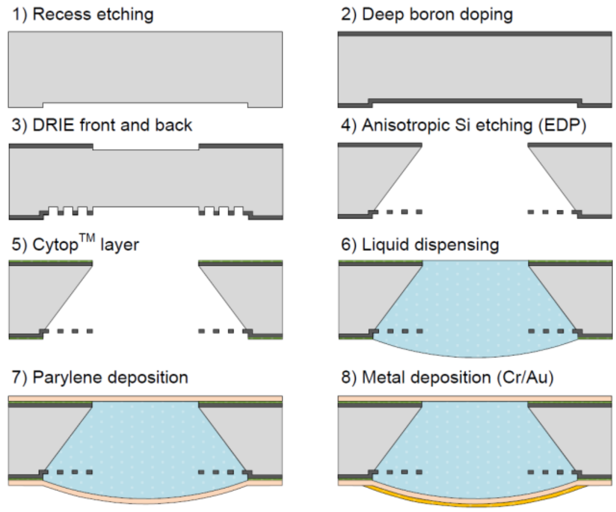

Figure 5: Fabrication process based on direct deposition of parylene over low vapor pressure silicone oil.

The final metal layer forming the second electrode is deposited through a shadow mask on the backside. Figure 6 shows fabricated electrostatic micro-hydraulic chips with perforated electrodes.

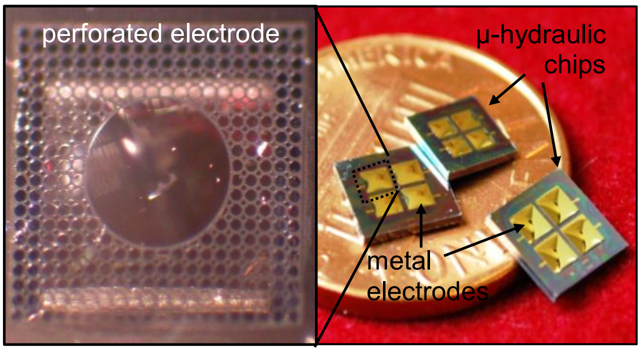

Figure 6: µ-hydraulic chips. Left: perforated membrane seen through Si-oil and parylene before metal deposition.

The silicon chip is mounted on a glass substrate that is recessed in selected areas to protect the backside membrane and provide interconnections (Figure 7). The recesses are deep enough to allow backside membranes to fully deflect at the full-scale force range. Using the glass substrate, we can directly wire bond to the device; wire bonding cannot be performed on substrates with parylene coating. The packaged device is shown in Figure 8.

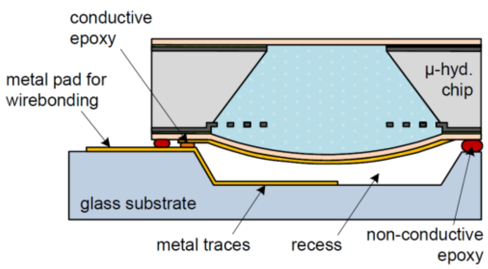

Figure 7: µ-hydraulic chip on top of recessed glass sub.

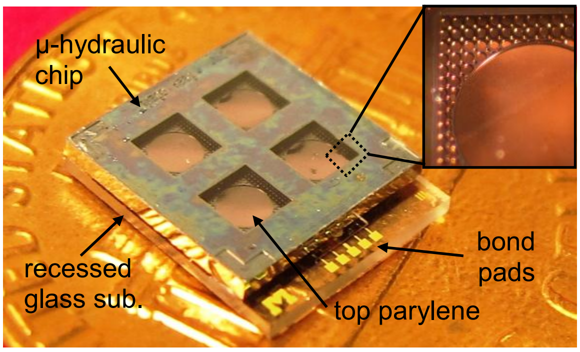

Figure 8: A packaged device including the glass chip and perforated electrode seen through top side parylene.

EXPERIMENTAL RESULTS

To characterize the fabricated micro-hydraulic structure, we mimicked sense mode operation by actuating the front-side with a piezoelectric beam actuator and measuring backside deflection by laser Doppler vibrometry (LDV). With this technique, we are able to measure the frequency response of the devices (Figure 9). The devices exhibit a maximum bandwidth of 70 Hz, which corresponds to an 18 ms sensor response time. Micro-hydraulic structures of various geometries show bandwidths of 50 to 70 Hz. The bandwidth range comes from variation in the center hole opening on the perforated electrode. A 50 Hz bandwidth corresponds to the smallest opening size (i.e. 55% of electrode diameter) while 70 Hz corresponds to the largest opening size (i.e. 65% of electrode diameter). This bandwidth is comparable to pneumatic and piezoelectric hydraulic devices which require external actuators [1, 6], while we have integrated the electrostatic sense/actuate element into our micro-hydraulic device.

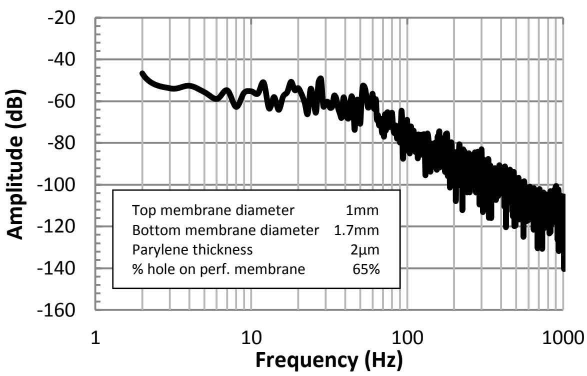

Figure 9: Frequency response of a fabricated sloped-wall device with perforated membrane, which shows bandwidth of about 70 Hz, equivalent to a response time of approximately 18 ms.

CONCLUSION

In this paper, we have introduced a novel high-speed micro-hydraulic structure. We have analyzed the dynamics of this system through simulation and used the results to develop a new architecture which reduces the response time of the sensor by several orders of magnitude. The micro-hydraulic structure is well suited for high performance sensing applications where wide dynamic range and high resolution are needed in a low power system. It can also be used for devices where large displacement actuation out of the plane of the substrate is needed. The new micro-hydraulic structures are successfully fabricated and tested. The devices offer a high measured bandwidth between 50 to 70 Hz, and based on simulations the rise and fall times should be symmetric. In the future, other fluids with low viscosity could be used to achieve even faster devices.

ACKNOWLEDGEMENTS

The authors thank Dr. Behrouz Shiari for modeling support, and Katherine Knisely and Karen Dowling for help in testing. Fabrication was performed at the Lurie Nano-fabrication Facility (LNF), a member of the NSF National Nanotechnology Infrastructure Network (NNIN). This project is funded by the MAST Program of the Army Research Lab under Award Number W911NF-08-2-0004.

REFERENCES

[1] M. De Volder and D. Reynaerts, "Pneumatic and Hydraulic Microactuators: A Review", *J. Micromech. & Microeng.,* vol. 20, 043001, March 2010.
[2] H. Kim, S. Lee, K. Najafi, "High-Force Liquid-Gap Electrostatic Hydraulic Micro Actuators", *Int. Conf. on Miniaturized Systems for Chemistry & Life Sciences, µTAS*, Paris, pp. 1735-1737, 2007.
[3] M. Sadeghi, H. Kim and K. Najafi, "Electrostatically Driven Micro-Hydraulic Actuator Arrays", *IEEE Int. MEMS Conf.*, Hong Kong, January 2010, pp. 15-18.
[4] M. M. Sadeghi, R. L. Peterson and K. Najafi, "Micro-Hydraulic Structure for High Performance Bio-Mimetic Air Flow Sensor Arrays", in *Tech. Digest IEDM,* Washington DC, December 5-7, 2011, pp. 673-676.
[5] M. M. Sadeghi, K. Dowling, R. L. Peterson and K. Najafi, "High Sensitivity, High Density Micro-Hydraulic Force Sensor Array Utilizing Stereo-Lithography Fabrication Technique", *IEEE Int. MEMS Conf.*, Taipei, January 20-24, 2013.
[6] T. Ninomiya, Y. Okayama, Y. Matsumoto, X. Arouette, K. Osawa, N. Miki, "MEMS-based Hydraulic Displacement Amplification Mechanism with Completely Encapsulated Liquid," *Sensors and Actuators A*, vol. 166, no. 2, pp. 277–282, April 2011.
[7] M. M. Sadeghi, R. L. Peterson and K. Najafi, "Hair-based Sensors for Micro-autonomous Systems", in *Proc. of the SPIE8373, Micro- and Nanotechnology Sensors, Systems and Applications IV,* Baltimore, April 23, 2012, paper 83731L.
[8] J. O. Wilkes, *Fluid Mechanics for Chemical Engineers*, *2nd ed.*, Prentice Hall, 2006.

CONTACT

K. Najafi, Tel: +1-734-763-6650, najafi@umich.edu
M. Sadeghi, Tel: +1-734-764-7428, sadeghi@umich.edu